euspen's 21st International Conference & Exhibition, Copenhagen, DK, June 2021

www.euspen.eu

Numerical analysis of magnetic bearings for micro machining applications

Andreas Lange[1], Daniel Müller[1], Benjamin Kirsch[1], Jan C. Aurich[1]

[1]*Technische Universität Kaiserslautern; Institute for Manufacturing Technology and Production Systems*

andreas.lange@mv.uni-kl.de

Abstract

The possibility to improve the accuracy of machine tool spindles through active control makes magnetic bearings an interesting option for high-frequency spindles used in micro machining. However, the required high speeds and accuracies necessitate a sophisticated design of the magnetic bearing and the control loop. Analytical models do not provide sufficient accuracy for this design, since nonlinear material behaviour, fringing effects and the exact geometric configuration of the magnetic bearing are not considered. While coupling finite element method (FEM) and control loop models provides sufficient accuracy, the recomputation of the FEM model at each time step is time consuming and therefore not suitable for controller optimization.

In this paper, a numerical model of a magnetic bearing spindle concept is developed and analysed. The bearing forces are initially computed using a FEM model and then converted to response surfaces. These response surfaces are then integrated in the time-dependent control loop. This eliminates the time-consuming recomputation of the FEM model while maintaining the same accuracy. Moreover, due to the time saved, the controller parameters can be optimized effectively.

The influence of nonlinear material behaviour, fringing effects, and the exact geometric configuration of the magnetic bearing on the magnetic bearing forces is investigated. For this purpose, the analytically calculated bearing forces are compared to the bearing forces computed with the numerical model with response surfaces. The comparison shows that for the same vibrational behaviour of the rotor, the numerically computed bearing forces are significantly lower than those calculated analytically. This is due to the fact that the analytical model does not represent the exact geometric configuration in sufficient detail. It can be concluded that the use of response surfaces for the integration of the bearing forces into the control loop allows a more detailed design and analysis of magnetic bearings.

Magnetic bearing, Finite Element Method (FEM), Vibration, Mechatronic

1. Introduction

Active magnetic bearings have already been successfully used in macro machining spindles to minimize tool-run out and to increase achievable rotational speeds [1, 2]. Investigations into the possibility of using magnetic bearings in high-frequency spindles for micro machining also exist [3]. However, the high precision and high speeds required in micro machining necessitate an exact electromagnetic model of the magnetic bearing for bearing design. Further, sophisticated tuning methods are necessary to select suitable control parameters.

The setup of a control loop model of a magnetic bearing usually consists of a model of the magnetic bearing itself and the control loop required for the active control of the bearing.

The magnetic circuit method is commonly used to model magnetic bearings within the control loop [4]. However, this method has the disadvantage of not considering relevant aspects such as fringing effects, nonlinear material behaviour, and the exact geometric configuration of the bearing.

Another possibility is the use of coupled finite element method (FEM) and control loop models [5]. Here, the FEM model is fully integrated in the control loop. The manipulated variable of the controller (electric currents) is used as the input parameter for the FEM model. The results of the FEM model (magnetic forces) are fed back into the control loop as the controlled variable. Such a coupled model provides sufficient accuracy, but the recomputation of the FEM model at each time step is time consuming and therefore not suitable for controller optimization.

In this paper, a control system model of a rotor, supported by an axial magnetic bearing and two radial magnetic bearings is set up, verified, analysed, and tuned. For this purpose, static magnetic finite element models of the bearings are set up to compute the magnetic forces. These bearing forces are then converted to response surfaces and integrated in a time-dependent control loop model of a magnetic bearing-rotor system. Using this model, the computed magnetic forces are compared against analytically calculated magnetic forces using the magnetic circuit method. Further, the controllers are tuned to reduce the vibration amplitude of the rotordynamics model.

2. Methods

The control loop model setup is conducted in two steps: the computation of the magnetic bearing forces using a static magnetic simulation model based on the FEM, and the setup of the control loop model itself including the response surfaces.

2.1. Finite element model setup

Three-dimensional static electromagnetic models of active magnetic axial and radial bearings are set up using ANSYS Mechanical[1]. A schematic view of the magnetic bearing-rotor configuration as well as the axial and radial bearings is given in figure 1. Both bearings are heteropolar 4-pole-pair active magnetic bearings featuring differential winding schemes to keep remagnetization of the rotor as low as possible upon rotation [4]. In this design, the remagnetization frequency is twice the rotation frequency. Half of the coils are operated with the sum and the

difference of the bias currents i_0 and control currents i_x and i_y respectively [4]. Figure 1c shows the half of the radial bearing operated with the sum of bias current and control current.

The nonlinear material behaviour of the iron core and the rotor is represented by B-H-curves which account for the magnetic saturation of the materials [4]. Fringing effects [4] are included by modelling the air region (air box) around the iron core (see figure 1c). The required boundary conditions are the number of turns, the conducting area, the current flow direction, the current through each coil, and the rotor position. In this paper, the axial bearing is assumed to be acting solely in z-direction, while the radial bearings only act in the x-y-plane. Thus, no coupling between axial and radial motion and no tilting of the rotor is considered in the electromagnetic model. Hysteresis losses due to remagnetization and eddy current losses due to velocity effects (angular velocity) are not considered.

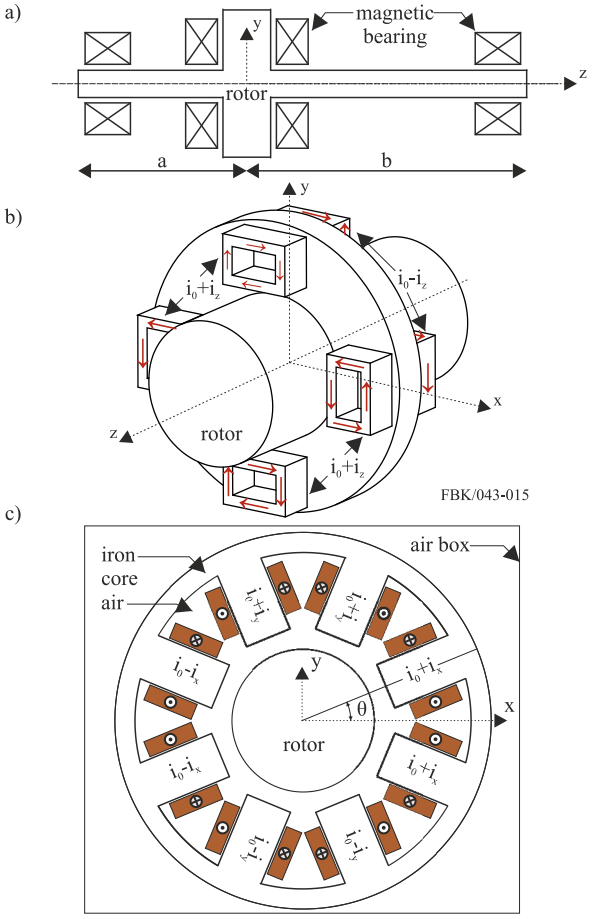

Figure 1. a) schematic view of the magnetic bearing-rotor configuration, b) and c) schematic view and applied boundary conditions of the magnetic axial and radial bearing model

The bearing models are solved using an edge-based magnetic vector potential method based on the Maxwell equations [6]. Bearing forces are computed using the Maxwell method [6]. For the axial bearing, the resulting magnetic force of interest is in z-direction, whereas the resulting magnetic force of interest for the radial bearings is in x- and y-direction.

2.2. Response surface generation

The magnetic bearing force is dependent on the input current and the position of the rotor. Hence, for the axial bearing, a two-dimensional response surface with the current i_z and the z-position of the rotor as inputs and the magnetic force in z-direction as the output is required. For a radial bearing, two four-dimensional response surfaces are required: one to represent the magnetic forces in x-direction and one to represent the forces in y-direction. For both response surfaces, the currents i_x and i_y, and the rotor position in both x- and y-direction are the inputs. The outputs are the magnetic forces in x- and y-direction.

2.3. Rotordynamics

A lumped mass approach is chosen to model the rotor's vibrational behaviour. This approach uses the centre of mass to compute dynamic effects. Thus, a total of six equations are required to describe the translational motion in x-, y- and z-direction, the tilting motion α and β along the x- and y-axis, and the rotational motion φ around the z-axis:

$$m\ddot{x} = -F_{x,1} - F_{x,2} + mg\sin\frac{\pi}{4} + m\varepsilon(\ddot{\varphi}\sin\varphi + \dot{\varphi}^2\cos\varphi) \quad (1)$$

$$m\ddot{y} = -F_{y,1} - F_{y,2} + mg\cos\frac{\pi}{4} + m\varepsilon(-\ddot{\varphi}\cos\varphi + \dot{\varphi}^2\sin\varphi) \quad (2)$$

$$m\ddot{z} = -F_{z,1} - F_{z,2} \quad (3)$$

$$J_d\ddot{\alpha} + \Omega J_p\dot{\beta} = -a \cdot f_{y,1} + b \cdot f_{y,2} \quad (4)$$

$$J_d\ddot{\beta} - \Omega J_p\dot{\alpha} = a \cdot f_{x,1} - b \cdot f_{x,2} \quad (5)$$

$$J_d\ddot{\varphi} = -F_{x,MB} \cdot (y + \varepsilon\sin\varphi) + F_{y,MB} \cdot (x + \varepsilon\cos\varphi) + M \quad (6)$$

where m is the rotor mass, ε is the rotor eccentricity, F_x and F_y are the magnetic bearing forces, g is gravity, φ is the rotational angle, $\dot{\varphi}$ is the rotational velocity, $\ddot{\varphi}$ is the rotational acceleration, J_d and J_p are the rotor's inertias around the x- and z-axis and M is the driving torque of the rotor. No coupling between axial and radial motion is considered.

2.4. Control system model setup

A time-dependent control system model is set up in Simulink[1] and shown in figure 2. Since no coupling between axial and radial motion of the rotor is considered here, the feedback loop of the axial magnetic bearing is a single-input single-output system (figure 2a)), whereas the feedback loop of the radial bearing is multiple-input multiple-output system (figure 2b)). Distributed proportional-integral-derivative (PID) controllers are employed to enable setpoint tracking. Additional feedbacks are set up to include the instantaneous rotational angle φ, the rotational velocity $\dot{\varphi}$, and the rotational acceleration $\ddot{\varphi}$ in the equations of motion. The model dynamics can be described as follows for a single time step: For a given driving torque M, the corresponding rotational speed is computed. The PID controllers determine the deviation of the rotor's instantaneous position from its setpoint position and accordingly alter the control currents i_x, i_y, i_z of the magnetic bearings. Based on the instantaneous values of the control currents and the rotor's position, the corresponding magnetic force is evaluated from the response surfaces. This updated magnetic force is passed to the equations of motion and used for the computation of the rotor's updated position.

2.5. Verification

Model verification is conducted by comparing results of magnetic flux density and magnetic force. For this purpose, the presented model is compared against an analytical model and a numerical reference model using a different electromagnetic simulation software (ANSYS Maxwell[1]).

The first verification test case is a U-shaped electromagnet [4]. The corresponding analytical formulas for the calculation of the magnetic flux density B and force f are as follows [4]:

$$B = \frac{\mu_0 \cdot n \cdot i}{2s} \quad (7)$$

$$f = \frac{1}{4}\mu_0 n^2 A_l \frac{i^2}{s^2} \quad (8)$$

where μ_0 is the vaccum permeability, n is the number of turns of a single coil, A_l is the pole face area, i is the current, and s is the air gap. Input data is chosen with reference to [7] and is as follows: $\mu_0 = 1.2566 \cdot 10^{-6}\ N/A$, $n = 460$, $A_l = 2.52 \cdot 10^{-4}\ m^2$, $i = 1\ A$, $s = 5 \cdot 10^{-4}\ m$.

The second verification test case is the actual radial bearing depicted in figure 1c.

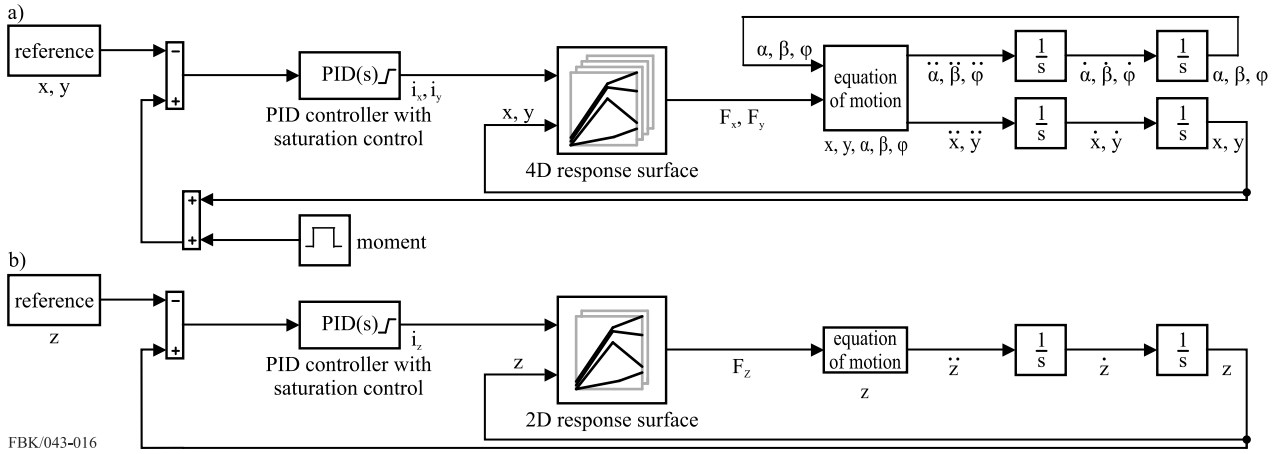

Figure 2. Control system model of a magnetic bearing-rotor system with an active magnetic axial bearing and two active magnetic radial bearings

For the radial bearing with differential winding scheme, the corresponding analytical formulas for the calculation of the magnetic flux density B_x and bearing force f_x in x-direction are given by [4]:

$$B_X = B_+ - B_- = \frac{1}{2}\mu_0 n\left(\frac{(i_0+i)}{(s_0+x)} - \frac{(i_0-i)}{(s_0-x)}\right)\cos\theta_x \qquad (9)$$

$$f_x = f_+ - f_- = \frac{1}{4}\mu_0 n^2 A_l\left(\frac{(i_0+i)^2}{(s_0+x)^2} - \frac{(i_0-i)^2}{(s_0-x)^2}\right)\cos\theta_x \qquad (10)$$

where i_0 is the bias current and θ_x is the angle between the magnet and the x-axis (see figure 1c). The magnetic flux density B_y and the electromagnetic force f_y in y-direction can be calculated similarly (with the angle $\theta_y = \theta_x$). Input data is as follows [7]: $n = 460$, $A_l = 2.52 \cdot 10^{-4}\ m^2$, $i_0 = 2\ A$, $i = 1\ A$, $\theta_x = 22.5°$, $s = 1 \cdot 10^{-3}\ m$, $\mu_0 = 1.2566 \cdot 10^{-6}\ N/A$.

Verification results are given in table 1. For the first verification test case, the ratio between the present model results, the numerical reference model results, and the analytical calculation results is close to 1, showing the good agreement between the presented model, the numerical reference model and the analytical calculation.

The results of the second verification test case show that while both numerical models are in good agreement with each other, the analytical formula is off by approximately 46 % and 80 % with regard to the numerically computed magnetic flux density and the magnetic force respectively. This is mainly due to the fact that the analytical formulas do not consider magnetic saturation. Further, the analytical formulas neglect fringing effects and are still based on a U-shaped magnet rotated about the x-axis and hence do not consider the exact geometric configuration.

Table 1. Comparison between computed magnetic bearing force and flux density of the presented model, a numerical reference model, and an analytical model

Geometry	Model	Bearing Force/N	Ratio	Flux density/T	Ratio
U-Magnet	Presented	173.75	-	0.62	-
	Numerical reference	176.90	0.98	0.61	1.01
	Analytical	163.36	1.06	0.63	0.98
4-pole-pair radial bearing	Presented	113.57	-	1.02	-
	Numerical reference	110.23	1.03	1.09	0.94
	Analytical	584.83	0.20	1.89	0.54

3. Results

To show the improved modelling accuracy and tuning capability of the control loop model with integrated response surfaces, an analysis of a magnetic bearing-rotor system, as shown in figure 1a, is conducted. Input data is as follows [7]: $s = 1 \cdot 10^{-3}\ m$, $\mu_0 = 1.2566 \cdot 10^{-6}\ N/A$, $A_l = 2.52 \cdot 10^{-4}\ m^2$, $\theta = 22.5°$, $\varepsilon = 3 \cdot 10^{-6}\ m$, $n = 460$, $J = 4.3 \cdot 10^{-4}\ kg\ m^2$, $i_0 = 2.5\ A$, $i = \pm 2.5\ A$.

3.1 Comparison of magnetic forces

The rotor motion can be divided into three segments: the lift-off phase where the rotor is brought into levitation (zero driving torque), the acceleration phase where the rotor is accelerated up to its nominal speed of $40{,}000\ rpm$ and the stationary phase with constant rotational velocity (zero driving torque).

Figure 3 shows a comparison of the numerically computed and analytically calculated magnetic bearing forces for the same vibrational behaviour of the rotor. The numerically computed forces (maximum value in lift-off phase: $172.96\ N$, in stationary phase: $26.18\ N$) are significantly lower than the analytically calculated forces (maximum value in lift-off phase: $194.45\ N$, in stationary phase: $40.88\ N$). This is due to the analytical model neglecting fringing effects, nonlinear material behaviour, and not considering the exact geometric configuration.

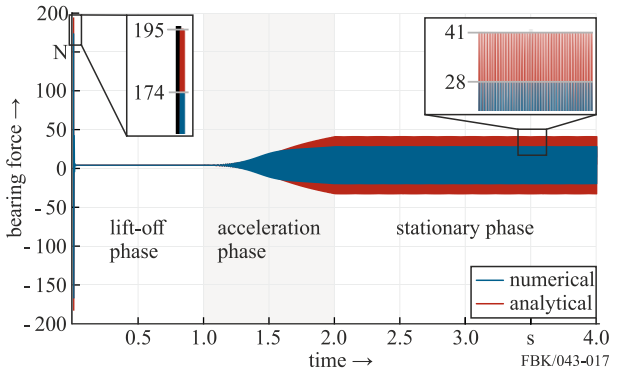

Figure 3. Numerically computed and analytically calculated forces

3.2 Tuning

Converting the input and output data of the presented finite element model to response surfaces and integrating those in the control system model allows for an efficient tuning of the PID controllers' gain values. Due to the required high precision and high rotational speeds of machine tool spindles for micro machining applications, manual tuning methods are time-consuming and not well suited. Hence, model-based automatic tuning methods are used to aid in the selection of suitable controller gain values. The single-input single-output system of the axial magnetic bearing is tuned using the Simulink PID Tuner app[1]. Figure 4 shows the initial and the tuned step responses of the axial magnetic bearing controller. Initial controller gain values were chosen with reference to [8]: $P = 10{,}000\ A/m$, $I = 15{,}000\ A/ms$, $D = 600\ As/m$. The tuned gain values are as

follows: $P = 3.546 \cdot 10^4\ A/m$, $I = 5.669 \cdot 10^6\ A/ms$, and $D = 54.460\ As/m$.

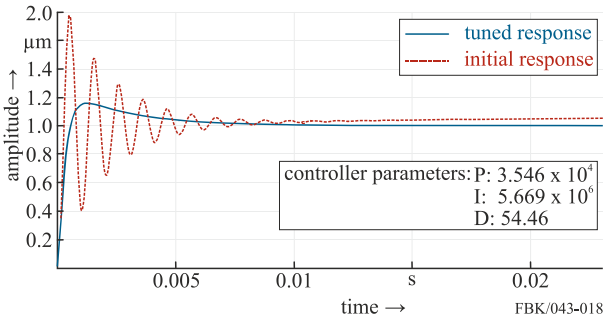

Figure 4. Initial and tuned step responses of the axial magnetic bearing

The tuned step response exhibits a smaller overshoot (16 % as opposed to 77 %) and no oscillatory behaviour. Additionally, the initial step response is not able to reach the desired target amplitude of 1 μm whereas the tuned response does after approximately 0.012 s.

The multiple-input multiple-output system of the radial magnetic bearings is tuned by simultaneously tuning both PID blocks using the Simulink Control System Tuner app[1]. For this purpose, the currents i_x, i_y, and i_z and the rotor's position in x-, y-, and z-direction are selected as the actor signals and sensor signals respectively. A comparison of the initial against the tuned radial rotor vibrations is shown in figure 5. The vibration amplitudes at the beginning of the simulation and in the stationary phase are shown enlarged. The initial controller gain values were chosen as follows [7]: $P_x = P_y = 7{,}200\ A/m$, $I_x = I_y = 55{,}800\ A/ms$, and $D_x = D_y = 194.7\ As/m$.

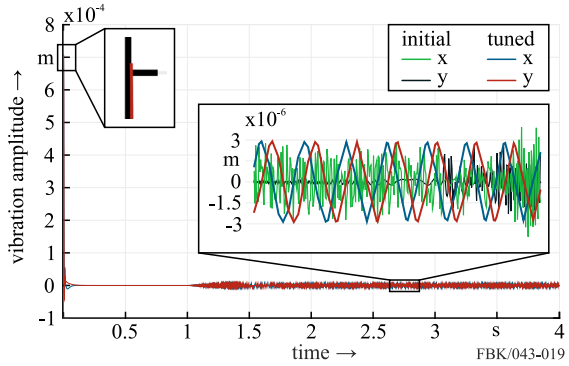

Figure 5. Initial and tuned radial rotor vibrations

Tuned controller gain values are: $P_x = P_y = 3{,}764\ A/m$, $I_x = I_y = 45{,}079\ A/ms$, and $D_x = D_y = 8.50\ As/m$.

The enlarged tuned vibration amplitude in the stationary phase shows the self-centering of the rotor, which can be observed in rotors that are operated (far) above their critical speed. Herein, the vibration amplitude corresponds exactly to the applied boundary condition, which is a rotating force due to mass unbalance with an eccentricity of 3 μm in this case. On the other hand, the initial rotor vibrations show high-frequency oscillations with an increased amplitude.

4. Conclusion and outlook

This paper investigated the suitability of modelling magnetic bearing forces using three-dimensional static magnetic finite element models depending on the rotor's position and the input current. After the solution of the finite element model, the computed magnetic forces were converted to response surfaces, correlating the finite element input signals (x, y, z, i_x, i_y, i_z) to the corresponding output forces (f_x, f_y, f_z). The response surfaces were used in a time-dependent control system model to investigate the difference in magnetic forces between the finite element model and an analytical model. The comparison showed that for the same vibrational behaviour of the rotor, the numerically computed bearing forces are significantly lower than those calculated analytically. Using the control system model with the integrated response surfaces, automatic tuning methods could be employed to reduce the rotor vibrations.

The following conclusions can be drawn from this analysis:

- Three-dimensional finite element models of magnetic bearings provide a better modelling accuracy than analytical methods based on the magnetic circuit method.
- Converting the input (geometry, currents, rotor position) and output data (magnetic forces) of the finite element model to response surfaces allows for an accurate representation of the magnetic forces without the need for a time-consuming recomputation of the FE model.
- The control system model with integrated response surfaces can be precisely tuned using model-based automatic methods. This would not be feasible if the full finite element model was implemented.
- A further reduction of the vibration amplitude, i.e. the compensation of the unbalance itself, is also possible with the aid of active magnetic bearings by adjusting the setpoint position itself as a function of speed and unbalance.

In future works, modified control system models will be set up, where the unbalance will be compensated, and the rotordynamics will be modelled using the finite element method to investigate the effects of coupled axial and radial motion. Further, hysteresis losses due to remagnetization will be computed and eddy current losses due to velocity effects will be included.

Acknowledgement

This research was funded by the Deutsche Forschungsgemeinschaft (DFG, German Research Foundation) – 252408385 – IRTG 2057.

[1]Naming of specific manufacturers is done solely for the sake of completeness and does not necessarily imply an endorsement of the named companies nor that the products are necessarily the best for the purpose.

References

[1] Chen M Knospe C R 2007 Control Approaches to the Suppression of Machining Chatter Using Active Magnetic Bearings: IEEE Transactions on Control Systems Technology **15/2** 220-232

[2] Jang H-D, Kim J, Han D-C, Jang D-Y and Ahn H-J 2012 Improvement of High-speed Stability of an Aerostatic Bearing-Rotor System Using an Active Magnetic Bearing: *International Journal of Precision Engineering and Manufacturing* **15/12** 2565-2572

[3] Kimman M H, Langen H H, Munnig Schmidt R H 2010 A miniature milling spindle with Active Magnetic Bearings: Mechatronics **20/2** 224-235

[4] Schweitzer G and Maslen E H 2009 Magnetic Bearings: Theory, Design, and Application to Rotating Machinery: *Springer Science & Business Media*

[5] Yang H, Zhao R X, Tang Q B 2006 Study on Inverter-fed Three-pole Active Magnetic Bearing: Twenty-First Annual IEEE Applied Power Electronics Conference and Exposition 1576-1581

[6] Jackson J D 1999 Classical electrodynamics: John Wiley & Sons, 3rd Edition

[7] Lange A, Müller D, Kirsch B, Aurich J C 2020 Magneto-structural modelling of micro machining spindles supported by active magnetic bearings: *euspen's 20th International Conference & Exhibition*

[8] Beitelschmidt, M, Dresig, H (Eds.) 2017 Maschinendynamik-Aufgaben und Beispiele. Springer Berlin Heidelberg